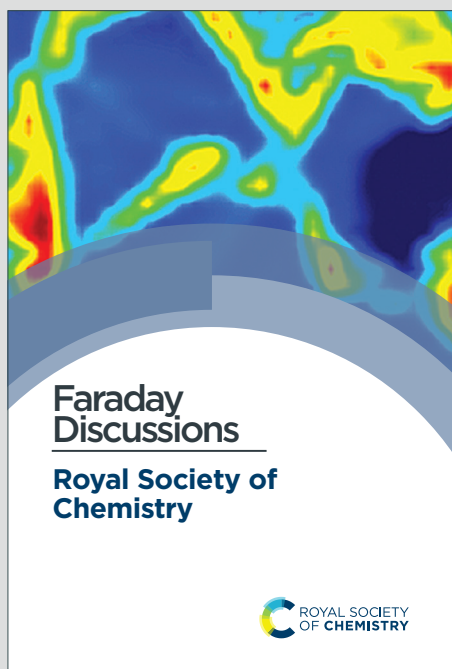


Faraday Discussions

Accepted Manuscript



This is an Accepted Manuscript, which has been through the Royal Society of Chemistry peer review process and has been accepted for publication.

Accepted Manuscripts are published online shortly after acceptance, before technical editing, formatting and proof reading. Using this free service, authors can make their results available to the community, in citable form, before we publish the edited article. We will replace this Accepted Manuscript with the edited and formatted Advance Article as soon as it is available.

You can find more information about Accepted Manuscripts in the [Information for Authors](#).

Please note that technical editing may introduce minor changes to the text and/or graphics, which may alter content. The journal's standard [Terms & Conditions](#) and the [Ethical guidelines](#) still apply. In no event shall the Royal Society of Chemistry be held responsible for any errors or omissions in this Accepted Manuscript or any consequences arising from the use of any information it contains.

This article can be cited before page numbers have been issued, to do this please use: N. N. Moghal, D. Giannantonio, M. R. Elliott, N. Mehta, A. P. Dove and A. Brandolese, *Faraday Discuss.*, 2025, DOI: 10.1039/D5FD00073D.

ARTICLE

On-demand manufacture of circular 3D printing resins

Nailah N. Moghal,^a Daniele Giannantonio,^a Megan R. Elliott,^a Neha Mehta,^b Andrew P. Dove,^{*a} Arianna Brandolese^{*a}

Received 00th January 20xx,
Accepted 00th January 20xx

DOI: 10.1039/x0xx00000x

Recent progress in circular 3D-printable photocurable resins that enable closed-loop recycling marks a significant step forward in reducing wasteful manufacturing methods and non-recyclable printed plastics. However, with 3D printing technologies shifting from prototyping to full-scale production, the demand for high-scale processes and easily tuneable resin compositions can benefit from the design of automated systems. Herein, we report on the on-demand preparation of a circular 3D printable resin, achieved through a continuous flow approach. A supported enzyme (Lipase B from *Candida antarctica*) was used to promote a green esterification of the lipoic acid with biobased alcohols to prepare circular biobased photocurable resins. The supported enzyme was employed for the preparation of a packed bed reactor and was easily recycled and reused to achieve the continuous production of lipoate-based photocurable resins with tuneable composition. Lastly, the environmental impact of the developed on-demand manufacture process was compared to the previously reported esterification protocols through life cycle assessment, showing the effectiveness of continuous enzymatic flow synthesis in enhancing environmental performance across multiple areas, from human health to ecosystem impact and resources.

Introduction

Vat photopolymerisation is a widely adopted additive manufacturing (3D printing) method that relies on light-activated polymerisation to selectively solidify liquid resins held in a vat.^{1,2} The additive manufacturing market, currently valued at \$0.9 billion, accounts for a significant share of the broader photopolymer market, which exceeds \$2.8 billion in total, and it is projected to expand at a compound annual growth rate of 16.9% as photopolymer-based 3D printing technologies become faster and shift from prototyping to full-scale production.³ However, this growth must be accompanied by advancements in photopolymer resin technology to ensure that additive manufacturing contributes to a truly sustainable and circular plastic economy.

Most resin components are derived from non-renewable fossil resources, and many resin-based processes generate waste in the form of partially cured material that cannot be reused.⁴⁻⁷ Additionally, the majority of 3D-printed objects made from permanently cross-linked resins are neither degradable nor recyclable, further exacerbating environmental damage and creating significant end-of-life challenges. To tackle this issue, closed-loop recycling of 3D-printed polymers, in which the printed material is fully depolymerised to a resin and re-printed, has been explored. Circular photocurable resins have been

focused on the introduction of dynamic bonds that can break down under certain conditions within permanently cross-linked polymer networks, allowing partial depolymerisation of printed parts.⁸⁻¹⁶ Recently, we reported on circular lipoate-based resins entirely obtained from renewable feedstocks that can be 3D-printed into high-resolution parts, efficiently deconstructed, and subsequently reprinted in a circular manner.¹¹ Yang *et al*, have also reported a circular additive manufacturing process to produce high-performance polymer parts containing dithioacetals bonds that can be decomposed into reprintable liquid resins under a specific condition.¹⁶

3D printing has been successfully employed to prepare sophisticated architectures in flexible devices and multimaterial objects that can have varied properties, including conductivity, self-healing capacity, and recyclability.¹⁷⁻¹⁹ Through vat photopolymerisation, it is possible to achieve the rapid production of customised 3D-printed components. Tuneable resins are conventionally formulated by varying the ratio of monomer manually^{20,21}, whereas the need to move to a large-scale production and the demand for precise control over resin composition can benefit from the design of automated systems. In this regard, the flow approach can be leveraged to develop an automated method to prepare photocurable resins with easily tuneable composition. Applying flow chemistry techniques to synthesis offers several advantages over traditional batch synthesis methods.²²⁻²⁵ Not only does it allow for greater repeatability and easier scale-up, but it can also be tuned to deliver bespoke products (*e.g.* resin with specific composition).^{26,27} While flow chemistry has largely benefited from the use of 3D printing (*e.g.* to print continuous flow reactors),²⁸ there have been no reports of using flow systems to directly synthesise photopolymer resins for 3D printing.

^a University of Birmingham, School of Chemistry, Edgbaston, B15 2TT, United Kingdom, E-mail: a.brandolese@bham.ac.uk, a.dove@bham.ac.uk

^b Birmingham Energy Institute, School of Chemical Engineering, University of Birmingham, Birmingham B15 2TT, UK

Supplementary Information available: [details of any supplementary information available should be included here]. See DOI: 10.1039/x0xx00000x



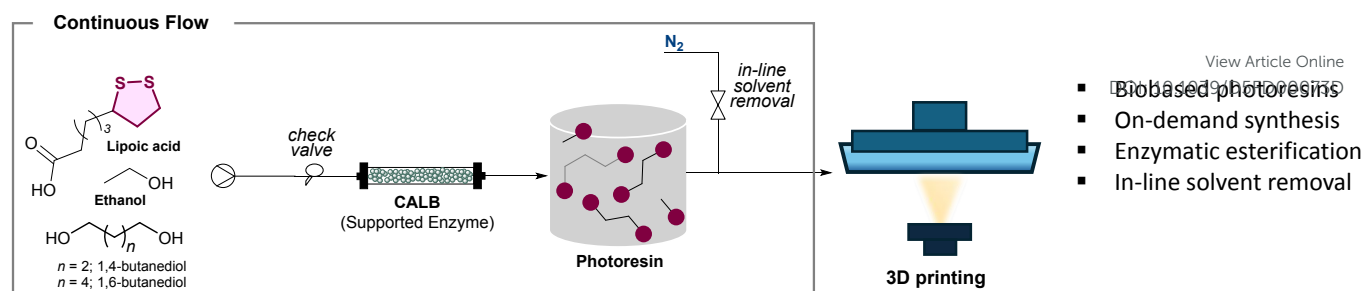


Figure 1. On-demand photocurable resin synthesis under continuous flow followed by off-line 3D printing developed in this work.

Herein, we report on the preparation of an on-demand circular biobased resin by leveraging continuous flow production (Figure 1). Lipoate-based photocurable resins have been synthesised using a sustainable enzymatic esterification. The environmental feasibility of the circular resin production under continuous flow was lastly assessed through life cycle assessment analysis, proving it to be a more sustainable strategy than the previously reported synthetic protocols.

Results and discussion

Enzymatic esterification under continuous flow

Liquid resin formulations employed in 3D printing are usually made of a reactive diluent and multivalent crosslinkers. The reactive diluent, ethyl lipoate (EtLp₁) synthesis was carried out under continuous flow (Table 1), exploring a range of solvents including dichloromethane (CH₂Cl₂), and greener ones, such as 2-methyl tetrahydrofuran (2-MeTHF) and methyl ethyl ketone (MEK). A single syringe system was used by combining ethanol (1.05 equiv.) and a solution of lipoic acid (LA) in CH₂Cl₂ (2.42 M). Initially, a packed bed reactor was prepared using 0.5 g of supported Lipase B from *Candida antarctica* (CALB), and the reagents were flowed at a flow rate of 0.1 mL min⁻¹, resulting in a residence time of 25 minutes (see SI for details). Fractions of the EtLp₁ product were collected at 1 h intervals, and their composition was monitored by ¹H NMR spectroscopy. Under these conditions, a 65% EtLp₁ yield was detected when the steady state was achieved (Table 1, entry 1). To minimise the amount of the solvent employed in the process, the concentration of the solution was doubled, however, that led to a gelation of the solution within the reactor, making that condition impracticable for the production of photocurable resins (Table 1, entry 2).

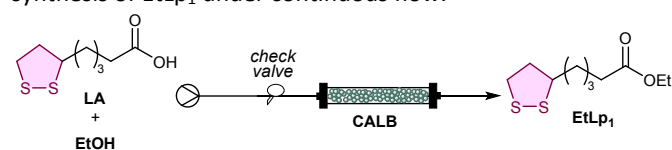
To increase the conversion of LA into the corresponding EtLp₁, catalyst amount and flow rate were then optimised. The catalyst amount was initially increased to 0.8 g, leading to an increased residence time of 35 mins. Under these conditions, an 88% EtLp₁ was obtained using 0.1 mL min⁻¹ flow rate (Table 1, entry 3). The results observed were consistent with previously reported experiments on continuous esterification, as conversion enhancement is seen with increasing the catalyst bed height.²⁹ A further increase in EtLp₁ yield (94%) was achieved by lowering the flow rate to 0.07 mL min⁻¹ (Table 1, entry 4).

With the aim of designing a sustainable and scalable esterification protocol, alternative green solvents with low boiling points were also explored. Use of 2-MeTHF as solvent resulted in a lower EtLp₁ yield (70%, Table 1, entry 5) at a 0.07 mL min⁻¹ flow rate, while a decrease to 0.05 mL min⁻¹ led to an EtLp₁ yield of 85% (Table 1, entry 6). The use of 2-MeTHF led to reduced process efficiency, most likely a consequence of its inferior resin swelling properties compared to CH₂Cl₂, which in turn resulted in less effective mass transfer (Figures S12 and S13). MEK was also tested, achieving 73% EtLp₁ formation at room temperature with a 0.07 mL min⁻¹ flow rate (entry 7, Figure S14). Decreasing the flow rate to 0.05 mL min⁻¹ showed no improvement (Table 1, entry 8).

To explore the process scalability, a large-scale reactor was prepared with 2 g of supported enzyme. The scale-up was tested using CH₂Cl₂, and the results achieved were consistent with the small-scale experiments (Table 1, entry 9). Moreover, the use of drying agents (*e.g.*, MgSO₄ or molecular sieves) to suppress ester hydrolysis during esterification yielded negligible improvement (Table 1, entry 10). Finally, to understand the stability of the developed system, a long-run experiment was performed. Fractions were collected every hour, and EtLp₁ formation was stable for 13 h, with more than 36 g of EtLp₁ produced in that timeframe (Figure 2a).

To explore the preparation of photocurable resins under flow, multivalent crosslinkers were then synthesised following the same protocol used for the reactive diluent, EtLp₁. Previously reported lipoic acid-based crosslinkers¹¹ were initially targeted. Glycerol and sugar-based isosorbide and isomanide were tested, however, their enzymatic esterification at room temperature was inefficient. Hence, alternative biobased alcohols, 1,4-butanediol and 1,6-butanediol, were considered.^{30, 31} The synthesis of the hexyl lipoate derivative (HexLp₂) was carried out by combining 1,6-hexandiol (1 equiv.) and a solution of LA in CH₂Cl₂ (2.42 M). Reagents were initially supplied at a flow rate of 0.1 mL min⁻¹ and fractions were collected at 1 h intervals and analysed by ¹H NMR spectroscopy. Under these conditions, HexLp₂ was obtained with an 86% yield (Figure 2b), while using a flow rate of 0.08 mL min⁻¹ was shown to lead only to a slightly higher yield (89%). Lastly, decreasing the flow rate to 0.05 mL min⁻¹ showed consistent data with higher flow rates, with only a marginal increase in yield (90% yield of HexLp₂).



Table 1. Screening of the reaction conditions for the enzymatic synthesis of EtLp₁ under continuous flow.^a

Entry	Catalyst / g	Solvent	Flow rate / mL min ⁻¹	τ / min	EtLp ₁ / %
1	0.5	CH ₂ Cl ₂	0.1	25	65
2 ^b	0.5	CH ₂ Cl ₂	0.1	25	/
3	0.8	CH ₂ Cl ₂	0.1	35	88
4	0.8	CH ₂ Cl ₂	0.07	50	94
5	0.8	2-MeTHF	0.07	40	70
6	0.8	2-MeTHF	0.05	65	85
7	0.8	MEK	0.07	50	73
8	0.8	MEK	0.05	80	72
9 ^c	2.0	CH ₂ Cl ₂	0.11	80	95
10 ^c	2.0 + (0.5g MgSO ₄)	CH ₂ Cl ₂	0.1	80	96

^a Reaction conditions: LA (1 equiv.), EtOH (1.05 equiv.), solvent (2.42 M), CALB (x g), flow rate, rt. ^b Solvent (4.85 M). ^c EtOH (1.20 equiv.). τ stands for residence time.

Subsequently, the synthesis of butyl lipoate ester (ButLp₂) was carried out in flow using the same conditions optimised for HexLp₂, by combining 1,4-butanediol (1 equiv.) and a solution of LA in CH₂Cl₂ (2.42 M). Using a large-scale reactor (with 2 g of supported enzyme) with a flow rate of 0.1 mL min⁻¹ led to ButLp₂ being obtained with an 84% yield when the steady state was reached (Figure 2c).

Photocurable resin preparation under continuous flow

Photopolymer resins were prepared by combining reactive diluent (EtLp₁) and multivalent crosslinker (HexLp₂ or ButLp₂) made by continuous flow enzymatic esterification (Figure 3a). EtLp₁ and HexLp₂ were both prepared under continuous flow in separate flow reactors, each packed with the supported enzyme (0.8 g) and initially set to a flow rate of 0.07 mL min⁻¹. The outlet of each reactor was connected at a T-junction, and the mixed photocurable resin was collected in a separating funnel. Nitrogen was bubbled through the collected solution while the resin was being prepared to ensure that the final product had minimal solvent content for the following printing process. Aliquots were taken at 1 h intervals and the ratios of EtLp₁, HexLp₂ and lipoic acid of the combined resin were determined by ¹H NMR spectroscopy. As lipoic acid is not fully converted into the ester derivative, we anticipated that the unreacted LA could be incorporated into the material when photocured.

To determine whether the composition of the resin could be tuned *via* continuous flow, the flow rate of the EtLp₁ process was increased from 0.07 mL min⁻¹ to 0.1 mL min⁻¹. It was hypothesised that increasing the flow rate would result in a higher amount of EtLp₁ as there would be a higher volume of EtLp₁ in the combined resin compared to HexLp₂. On the other hand, increasing the flow rate would also increase the amount

of lipoic acid in the final photocurable resin as a lower conversion of EtLp₁ would be achieved with the lower residence time. The resulting resin composition showed that increasing the flow rate of EtLp₁ does lead to an increase in the amount of EtLp₁ and lipoic acid in the final resin and a decrease in the amount of the crosslinker HexLp₂ (Figure 3b). In doing so, we demonstrated that changing the continuous flow parameters enables the final resin composition to be tuned. This represents a novel approach to tune photocurable resin compositions and therefore prepare on-demand tailored photocurable resins in an automated way.

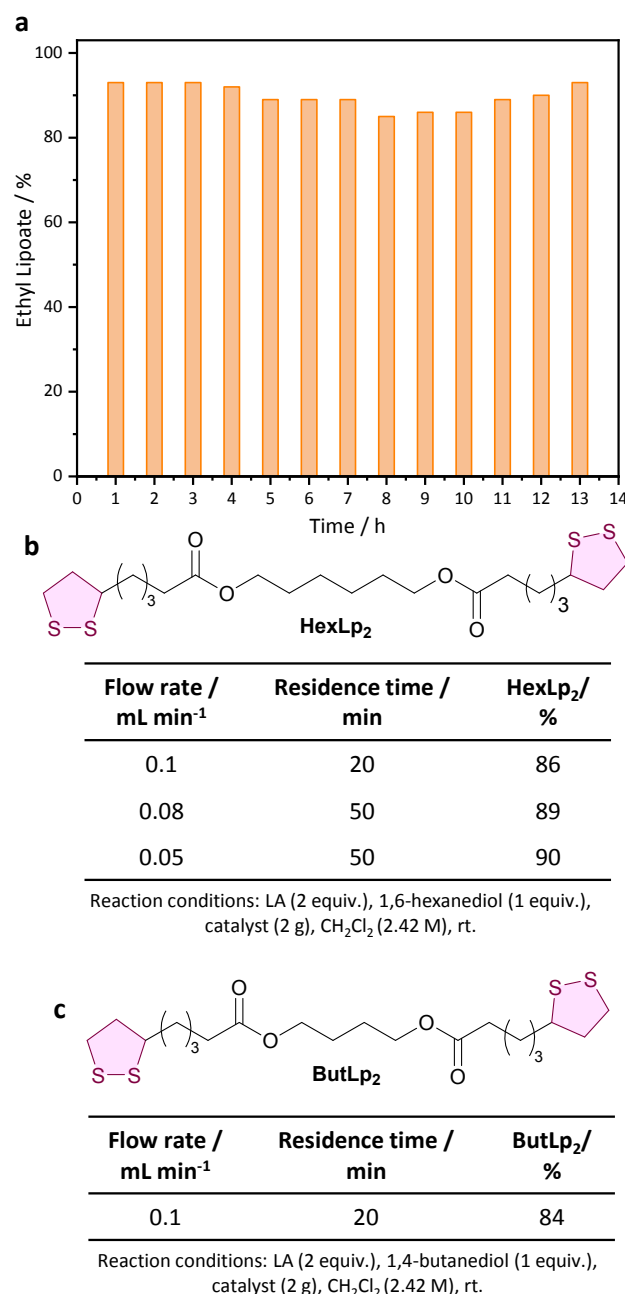


Figure 2. a. EtLp₁ long-run continuous flow preparation (reaction conditions Table 1, entry 4). b. Screening of the reaction conditions for the enzymatic synthesis of multivalent crosslinkers HexLp₂. c. Reaction conditions for the enzymatic synthesis of multivalent crosslinkers ButLp₂.



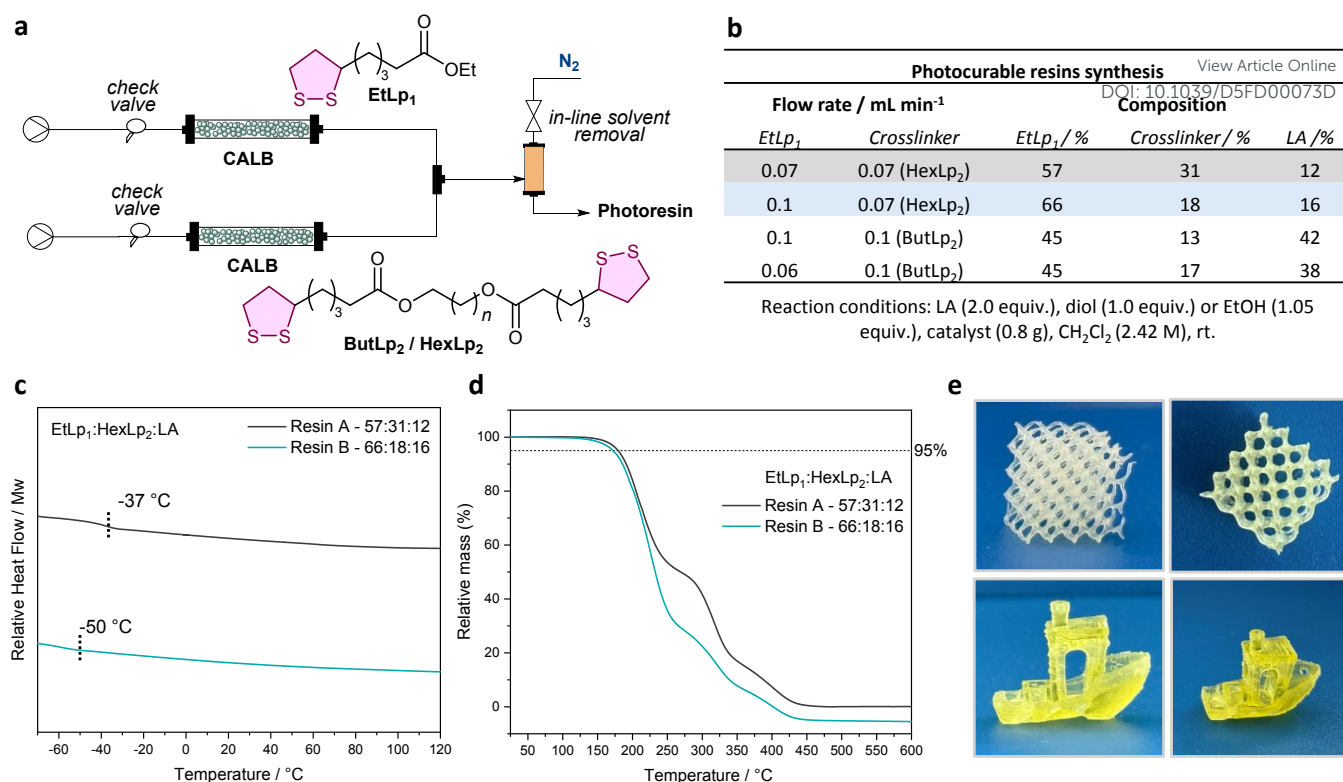


Figure 3. **a.** Continuous flow set-up for photocurable resin preparation. **b.** Composition of the combined photocurable resin obtained under continuous flow. **c.** DSC thermograms of the second heating cycle of EtLp₁:HexLp₂ resins (−80 to 130 °C, 10 °C min^{−1} under N₂), the *T_g* is indicated by the dashed line. **d.** TGA thermograms of EtLp₁:HexLp₂ resin 2D-photoset post-cured samples (25 – 600 °C, N₂ atmosphere). *T_{d5%}* is indicated by a horizontal line. **e.** 3D printed complex parts, top and front views.

Similarly, EtLp₁:ButLp₂:LA photocurable resin was prepared with an analogous set-up. Due to the higher flow rates employed relative to the EtLp₁:HexLp₂ resin preparation, the EtLp₁:ButLp₂ resin exhibited an increased lipoic acid content (Figure 3b). This outcome was anticipated as higher flow rates result in lower conversions.

To explore the material properties of the EtLp₁:HexLp₂:LA photopolymer resins, 2D photosets of the resins were prepared by curing 0.1 mL of resin on glass slides (10 min UV irradiation), followed by post-curing for 24 h at 60 °C (Figure S15). Differential scanning calorimetry (DSC) and thermogravimetric analysis (TGA) of the obtained photocured polymers were conducted. The glass transition temperature (*T_g*) for resin containing 57:31:12 ratio of EtLp₁: HexLp₂: LA (resin A) was −37 °C, whereas the *T_g* for resin containing 66:18:16 ratio of EtLp₁: HexLp₂: LA (resin B) was −50 °C (Figure 3c). The difference in *T_g* can be ascribed to the higher content of HexLp₂ crosslinker, which leads to a higher degree of crosslinking. This proof-of-concept experiment shows that the material properties of the resins can be tuned by preparing the photopolymer resins in flow. Lastly, both resins showed thermal stability up to 170 °C (Figure 3d), in line with lipoic acid-based photopolymers previously reported.¹¹

To explore the structure-property space of the platform, additional samples of the resin were prepared using ButLp₂.

However, we observed a partial gelation of the formulated photocurable resin as soon as the solvent was removed, which proved to be unsuitable for the following application in additive manufacturing.

Printing the resin EtLp₁: HexLp₂: LA (57:31:12) on a commercial digital light processing (DLP) printer was achieved using a λ = 405 nm light source (Figure 3e). The high-fidelity, complex prints were obtained using 35 s cure per layer, which corresponds to a build rate of 5.1 mm h^{−1} (excluding the peeling time process), demonstrating that the resins prepared through the continuous flow method remained suitable for DLP printing.

Life cycle assessment and green chemistry metrics

A first estimation of the sustainability of the preparation of circular lipoic acid-based resins was explored using green chemistry metrics (Table S1). The enzymatic reaction is considered to be a more sustainable approach, with chemicals such as *N*-(3-dimethylaminopropyl)-*N*'-ethylcarbodiimide (EDC), commonly used in esterification reactions, replaced by the supported enzyme. Additionally, the continuous flow approach minimises the purification process, limiting it to the sole solvent removal. For the proposed enzymatic process, the atom economy (AE)³² was equal to 93, meaning that most of the reagents are converted into the products with little waste production. In contrast, the previously



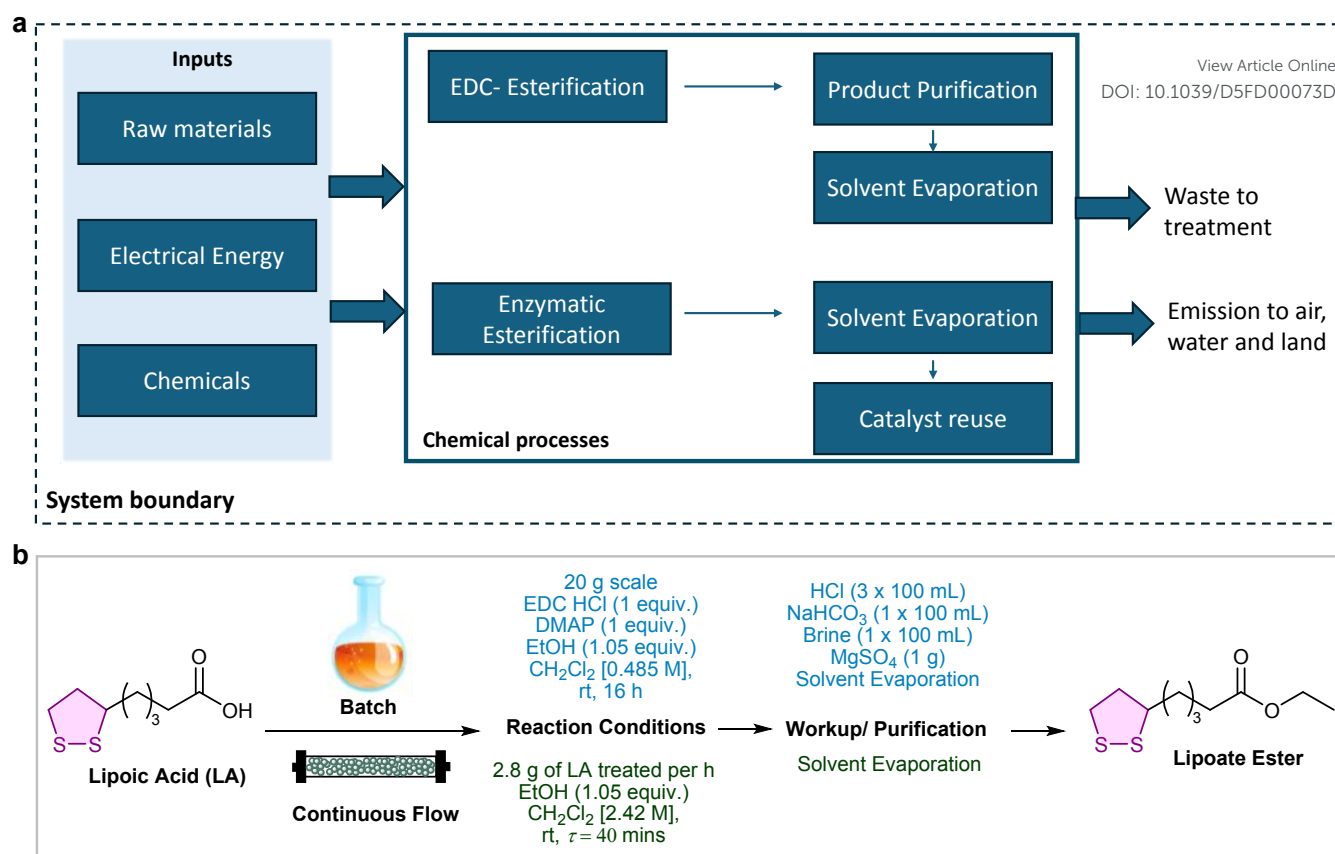


Figure 4. a. System boundary for life cycle analysis of lipoic acid esterification. **b.** Materials flow scheme for reaction procedure for both the petrochemical esterification under batch and enzymatic esterification under continuous flow, divided into two phases by reaction and workup/purification.

used EDC coupling¹¹ pathway (here named as petrochemical process) resulted in a significantly lower value as a consequence of the high amount of waste produced and the lower efficiency of the process (78% yield for the petrochemical process vs 94% for the enzymatic process). The *E* factor³³ for the enzymatic process was calculated to be < 0.01, falling into the range of oil refinery processes, while it is equal to 2.57 when the solvent is considered, showing a comparable value with the recently reported Fisher esterification process.³⁴ The use of EDC led to higher *E* factor (17.04 when the solvent is considered, Table S1), comparable with those of bulk processes. While these parameters showed that the enzymatic process presents a higher sustainability than the petrochemical one, an absolute assessment of the process sustainability must take into account the energy required for the reaction, as well as the impact of the production of the chemicals that are needed for the reactions themselves. Hence, to obtain a comprehensive understanding of the real sustainability of both reaction pathways, a life cycle assessment (LCA) that compares the two synthetic protocols was performed.

The LCA carried out conformed to the existing ISO standard (14044) and followed the typical LCA framework.³⁵ The LCA system boundary consisted of raw material and chemical supply, and electricity (Figure 4a). Material and chemical flows are depicted according to these

working schemes (Figure 4b). Outputs were not reused; all outputs were either transferred to the next process or, if not intended, considered as waste. The waste products from the system included byproducts, aqueous solutions and solid waste for which the impacts were not considered.

This LCA has a cradle-to-gate attributional approach and did not include any infrastructure processes related to lab equipment production (see SI for details). The background data used for basic chemicals, such as solvents, reagents, comes from the Ecoinvent-3 database. Lipoic acid is not included in the Ecoinvent-3 database used, therefore, it was replaced with the fatty acid, stearic acid. The amount of ester obtained for the petrochemical and enzymatic processes was obtained from experimental data, and the reaction conditions were adjusted to synthesise 100 g of ethyl ester. The petrochemical process was divided into two subprocesses, the synthetic one and the purification step. The enzymatic process instead did not require any purification, aside from solvent removal under vacuum and was therefore considered as a sole process. Finally, we considered the flow system to operate for 35 h to allow the preparation of 100 g of ethyl ester, assuming a steady state regime.



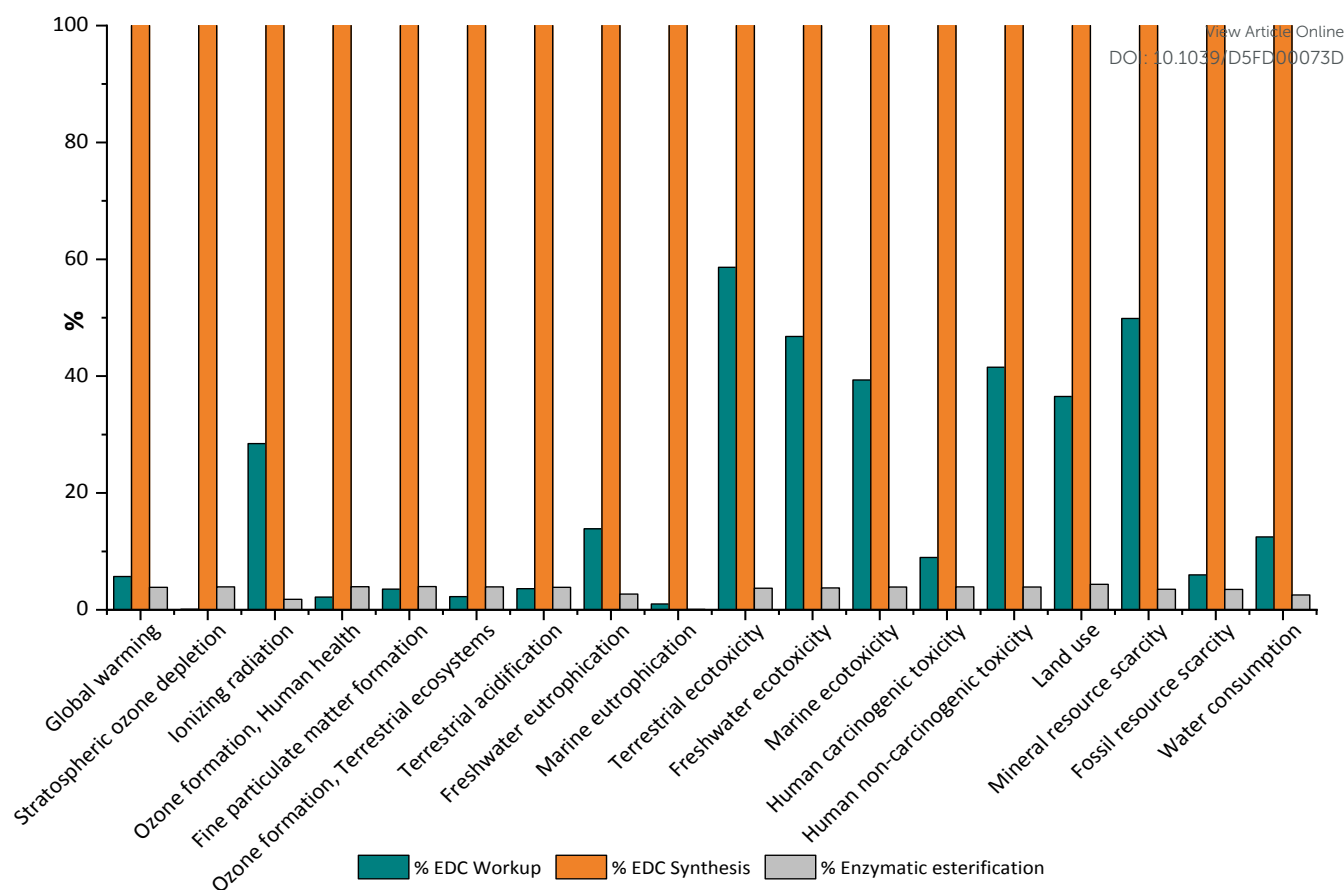


Figure 5. Environmental impacts due to the synthesis of 100 g of ethyl ester computed using ReCiPe 2016 V1.08.

In this study, midpoint indicator assessment was conducted using ReCiPe 2016 Endpoint (E) V 1.08 to better understand and compare the impact categories.³⁶ LCA of petrochemical esterification was conducted based on two stages in the inventory analysis: the synthetic process and the purification (removal of unreacted reagents and byproducts) process. The waste treatment processes and emissions to air, water and land were not considered as part of LCA.

Relative results were generated from the simulation for which the indicator results maximum is set to 100% (Figure 5 and Table S3). The petrochemical synthetic process is above the purification process in all the categories. When compared to the enzymatic process, the petrochemical synthesis is still above the purification and the enzymatic synthesis in all categories.

The petrochemical esterification process had the highest environmental impact across all criteria, mainly due to its long reaction time, high solvent use, and toxic reagents like EDC. The workup stage also contributed significantly, primarily through waste generation. In contrast, the enzymatic process showed the lowest impact, benefiting from a biobased catalyst, lower energy use, and more concentrated solutions that reduced solvent removal energy demands. Water consumption in the petrochemical process was 0.099 m³ per unit of product, while the continuous flow method used only 0.002 m³, reducing water usage by over 90% thanks to more

efficient reagent use and simpler purification. Land system changes were also significantly lower in the continuous flow process (0.002 m² vs. 0.061 m² per unit), mainly due to reduced solvent and reagent requirements. Carbon emissions were over 95% lower in the enzymatic process compared to the petrochemical route, highlighting the environmental benefits of using a syringe pump instead of a stirring plate. Across all nine planetary boundaries, including ocean acidification, biosphere integrity, and freshwater use the enzymatic approach showed the least impact. The petrochemical method had the highest toxicity, largely due to chlorinated reagents and solvents.

Lastly, ReCiPe 2016 Endpoint (E) V1.08 was used to conduct endpoint analysis. Human health, ecosystem quality and resources endpoint indicator assessments have been compared for the petrochemical and enzymatic process (Figure 6). Ecosystem quality comprises of acidification, ecotoxicity, eutrophication and land use (indicated as species*year (species*yr)). Human health is related to the impacts of environmental degradation that increases of, and duration of loss of life-related diseases (recorded as Disability-adjusted life year (DALY)). For resources, it is closely related to the depletion rate of raw materials and energy sources (recorded as extra costs in US dollars for future mineral and fossil resource extraction (USD)). Results are evaluated based on the future energy surplus



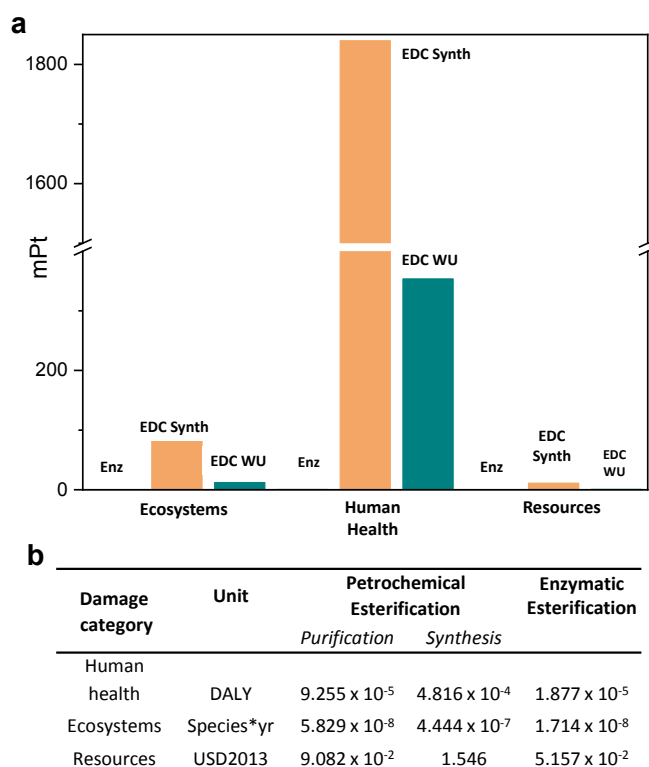


Figure 6. a. ReCiPe 2016 Endpoint (E) V1.08 endpoint indicators for producing 100 g of ethyl ester. *Enz* stands for enzymatic synthesis, *EDC synth* stands for petrochemical synthesis, and *EDC WU* represents the workup step for the petrochemical esterification. **b.** Environmental impacts due to the stearic acid esterification process (100 g) computed using ReCiPe 2016 Endpoint (E) V1.08.

requirements needed to produce lower-quality energy and minerals. For all the categories, the enzymatic esterification showed a lower impact than the petrochemical process (Figure 6b). By combining the precise Midpoint results with the aggregated Endpoint outcomes, we provided a robust and comprehensive assessment of the environmental performance of the seven processes, capturing both detailed category-specific impacts and their broader environmental effects. In summary, the implementation of the enzymatic esterification under continuous flow resulted in the reduction of more than 90% based on the average outcomes observed in the respective categories of the Endpoint method.

Conclusions

These results demonstrate a proof-of-concept advancement in developing a continuous flow system for the sustainable production of circular, biobased photocurable resins. Enzymatic esterification under continuous flow conditions enabled the on-demand synthesis of lipoate-based photocurable resins with tuneable compositions. The integration of in-line solvent removal streamlined the process, yielding one-step, printable resins that can be directly utilised in DLP printing. By employing renewable, sustainable, and non-hazardous lipoates, this approach effectively overcomes major limitations of current state-of-the-art resins and demonstrates significant

potential for broader implementation. Finally, the sustainability of the method was further assessed through life cycle analysis. Overall, the study reaffirms the effectiveness of continuous enzymatic flow synthesis in enhancing environmental performance across multiple areas, from human health to ecosystem impact and resources. Future work will focus on expanding the library of on-demand photocurable resins and developing an integrated one-pot online printing process.

Author contributions

A.B. and A.P.D. conceived the work. All authors designed the experiments. N.N.M., D.G., M.R.E. and A.B. performed and analysed experiments. N.M. aided in the LCA analysis. A.B. directed the research and prepared the manuscript. All authors contributed to manuscript revisions and have given approval to the final version of the manuscript.

Conflicts of interest

There are no conflicts to declare.

Data availability

The data supporting this article have been included as part of the Supplementary Information.

Acknowledgements

The authors acknowledge the University of Birmingham for support. Dr. Deborah Crawford is acknowledged for the helpful discussion about LCA analysis.

Notes and references

1. F. Zhang, L. Zhu, Z. Li, S. Wang, J. Shi, W. Tang, N. Li and J. Yang, *Additive Manufacturing*, 2021, **48**, 102423.
2. S. C. Ligon, R. Liska, J. Stampfl, M. Gurr and R. Mülhaupt, *Chemical reviews*, 2017, **117**, 10212-10290.
3. <https://www.grandviewresearch.com/industry-analysis/photopolymers-market-report>.
4. I. Gibson, D. Rosen, B. Stucker, M. Khorasani, D. Rosen, B. Stucker and M. Khorasani, *Additive manufacturing technologies*, Springer, 2021.
5. V. S. Voet, J. Guit and K. Loos, *Macromolecular rapid communications*, 2021, **42**, 2000475.
6. W. Li, L. S. Mille, J. A. Robledo, T. Uribe, V. Huerta and Y. S. Zhang, *Advanced healthcare materials*, 2020, **9**, 2000156.
7. M. Bachmann, C. Zibunas, J. Hartmann, V. Tulus, S. Suh, G. Guillén-Gosálbez and A. Bardow, *Nature Sustainability*, 2023, **6**, 599-610.
8. X. Lopez de Pariza, O. Varela, S. O. Catt, T. E. Long, E. Blasco and H. Sardon, *Nature communications*, 2023, **14**, 5504.
9. P. Chakma and D. Konkolewicz, *Angewandte Chemie International Edition*, 2019, **58**, 9682-9695.



Journal Name

ARTICLE

10. G. Zhu, H. A. Houck, C. A. Spiegel, C. Selhuber-Unkel, Y. Hou and E. Blasco, *Advanced Functional Materials*, 2024, **34**, 2300456.
11. T. O. Machado, C. J. Stubbs, V. Chiaradia, M. A. Alraddadi, A. Brandolese, J. C. Worch and A. P. Dove, *Nature*, 2024, **629**, 1069-1074.
12. B. Zhang, K. Kowsari, A. Serjouei, M. L. Dunn and Q. Ge, *Nature communications*, 2018, **9**, 1831.
13. M. Podgórski, S. Huang and C. N. Bowman, *ACS Applied Materials & Interfaces*, 2020, **13**, 12789-12796.
14. H. Gao, Y. Sun, M. Wang, Z. Wang, G. Han, L. Jin, P. Lin, Y. Xia and K. Zhang, *ACS Applied Materials & Interfaces*, 2020, **13**, 1581-1591.
15. J. J. Hernandez, A. L. Dobson, B. J. Carberry, A. S. Kuentler, P. K. Shah, K. S. Anseth, T. J. White and C. N. Bowman, *Macromolecules*, 2022, **55**, 1376-1385.
16. B. Yang, T. Ni, J. Wu, Z. Fang, K. Yang, B. He, X. Pu, G. Chen, C. Ni and D. Chen, *Science*, 2025, **388**, 170-175.
17. E. Yang, S. Miao, J. Zhong, Z. Zhang, D. K. Mills and L. G. Zhang, *Polymer Reviews*, 2018, **58**, 668-687.
18. S. Subedi, S. Liu, W. Wang, S. A. Naser Shovon, X. Chen and H. O. T. Ware, *npj Advanced Manufacturing*, 2024, **1**, 9.
19. A. Jadhav and V. S. Jadhav, *Materials Today: Proceedings*, 2022, **62**, 2094-2099.
20. R. Tu and H. A. Sodano, *Additive Manufacturing*, 2021, **46**, 102180.
21. C. C. Cook, E. J. Fong, J. J. Schwartz, D. H. Porcincula, A. C. Kaczmarek, J. S. Oakdale, B. D. Moran, K. M. Champley, C. M. Rackson and A. Muralidharan, *Advanced Materials*, 2020, **32**, 2003376.
22. N. Zaquen, M. Rubens, N. Corrigan, J. Xu, P. B. Zetterlund, C. Boyer and T. Junkers, *Progress in Polymer Science*, 2020, **107**, 101256.
23. A. Laybourn, K. Robertson and A. G. Slater, *Journal of the American Chemical Society*, 2023, **145**, 4355-4365.
24. S. B. Patterson, R. Wong, G. Barker and F. Vilela, *Journal of Flow Chemistry*, 2023, **13**, 103-119. DOI: 10.1039/D5FD00073D
25. M. H. Reis, F. A. Leibfarth and L. M. Pitet, *ACS Macro Letters*, 2020, **9**, 123-133.
26. M. B. Plutschack, B. u. Pieber, K. Gilmore and P. H. Seeberger, *Chemical reviews*, 2017, **117**, 11796-11893.
27. F. Fanelli, G. Parisi, L. Degennaro and R. Luisi, *Beilstein Journal of Organic Chemistry*, 2017, **13**, 520-542.
28. M. B. Montaner and S. T. Hilton, *Current Opinion in Green and Sustainable Chemistry*, 2024, 100923.
29. Y. Feng, A. Zhang, J. Li and B. He, *Bioresource Technology*, 2011, **102**, 3607-3609.
30. H. Kim, S. Lee and W. Won, *Energy*, 2021, **214**, 118974.
31. H. Guo, H. Liu, Y. Jin, R. Zhang, Y. Yu, L. Deng and F. Wang, *Biochemical Engineering Journal*, 2022, **185**, 108478.
32. P. Anastas and N. Eghbali, *Chemical Society Reviews*, 2010, **39**, 301-312.
33. R. A. Sheldon, *Green Chemistry*, 2007, **9**, 1273-1283.
34. C. Koelbl, C. Obunadike, W. Ham, N. Mahmud, M. Garcia, E. Lizundia and J. C. Worch, *ChemSusChem*, 2024, e202500194.
35. I. Iso, *Environmental management—life cycle assessment—requirements and guidelines*, 2006, 1-46.
36. M. A. Huijbregts, Z. J. Steinmann, P. M. Elshout, G. Stam, F. Verones, M. Vieira, M. Zijp, A. Hollander and R. Van Zelm, *The international journal of life cycle assessment*, 2017, **22**, 138-147.



View Article Online
DOI: 10.1039/D5FD00073D

Open Access Article. Published on 06 June 2025. Downloaded on 8/2/2025 6:41:57 AM.
This article is licensed under a Creative Commons Attribution 3.0 Unported Licence.



Faraday Discussions Accepted Manuscript

Data availability statement

[View Article Online](#)
DOI: 10.1039/D5FD00073D

The data supporting this article have been included as part of the Supplementary Information

